Supplementary material

Re-refinement of the Mm-MIOX structure

Attempts to re-refine the deposited 2HUO file failed initially due to the high anisotropy of the data (~2.8 Å resolution in the c* direction) and the inherent instability of TLS refinement as implemented in REFMAC5 (1). However, after applying an anisotropy correction as described in Strong *et al.* (2) and removing the solvent model it was possible to perform refinement using the PHENIX package (3). After a few rounds of refinement in PHENIX, a new TLS-model was introduced based on TLSMD analysis (4). The N-terminus was rebuilt in the improved density using COOT (5) and the model was extended with the sidechain of Phe^{28} that was now clearly visible. The main remodelling was however of the position of the backbone NH of Arg^{29}. This entity forms a strong ionic interaction with Asp^{90} (Fig. 2C in the main paper) but in 2HUO this NH-group was pointing outwards toward bulk water. Furthermore, the solvent model was rebuilt and a few sidechains were moved to their closest rotamer. The re-refined model belong to the upper 95^{th} percentile in overall quality in the resolution range 1.75-2.25 Å (12522 structures) according to Molprobity (6) (2HUO belong to the upper 47^{th} percentile).

1. Murshudov, G. N., Vagin, A. A., and Dodson, E. J. (1997) *Acta Crystallogr*. **D53**, 240-255

2. Strong, M., Sawaya, M.R., Wang, S., Phillips, M., Cascio, D. & Eisenberg, D. (2006). *PNAS*. **103**, 8060-3065

3. Adams, P.D., Grosse-Kunstleve, R.W., Hung, L.W., Ioerger, T.R., McCoy, A.J., Moriarty, N.W., Read, R.J., Sacchettini, J.C., Sauter & N.K., Terwilliger, T.C. (2002) *Acta Crystallogr*. **D58**, 1948-1954

4. Painter, J. & Merritt, E.A. (2006) *Acta Crystallogr*. **D62**, 439-450

5. Emsley, P., and Cowtan, K. (2004) *Acta Crystallogr*. **D60**, 2126-2132

6. Lovell, S.C., Davis, I.W., Arendall, W.B. 3rd, de Bakker, P.I., Word, J.M., Prisant, M.G., Richardson, J.S. and Richardson, D.C. (2003) *Proteins* **50**, 437-450.

7. Read, R.J. (1986) Acta Crystallogr. **A42**, 140-149.

Figure S1. Structure-based sequence alignment of 8 eukaryotic *myo*-Inositol oxygenase sequences.

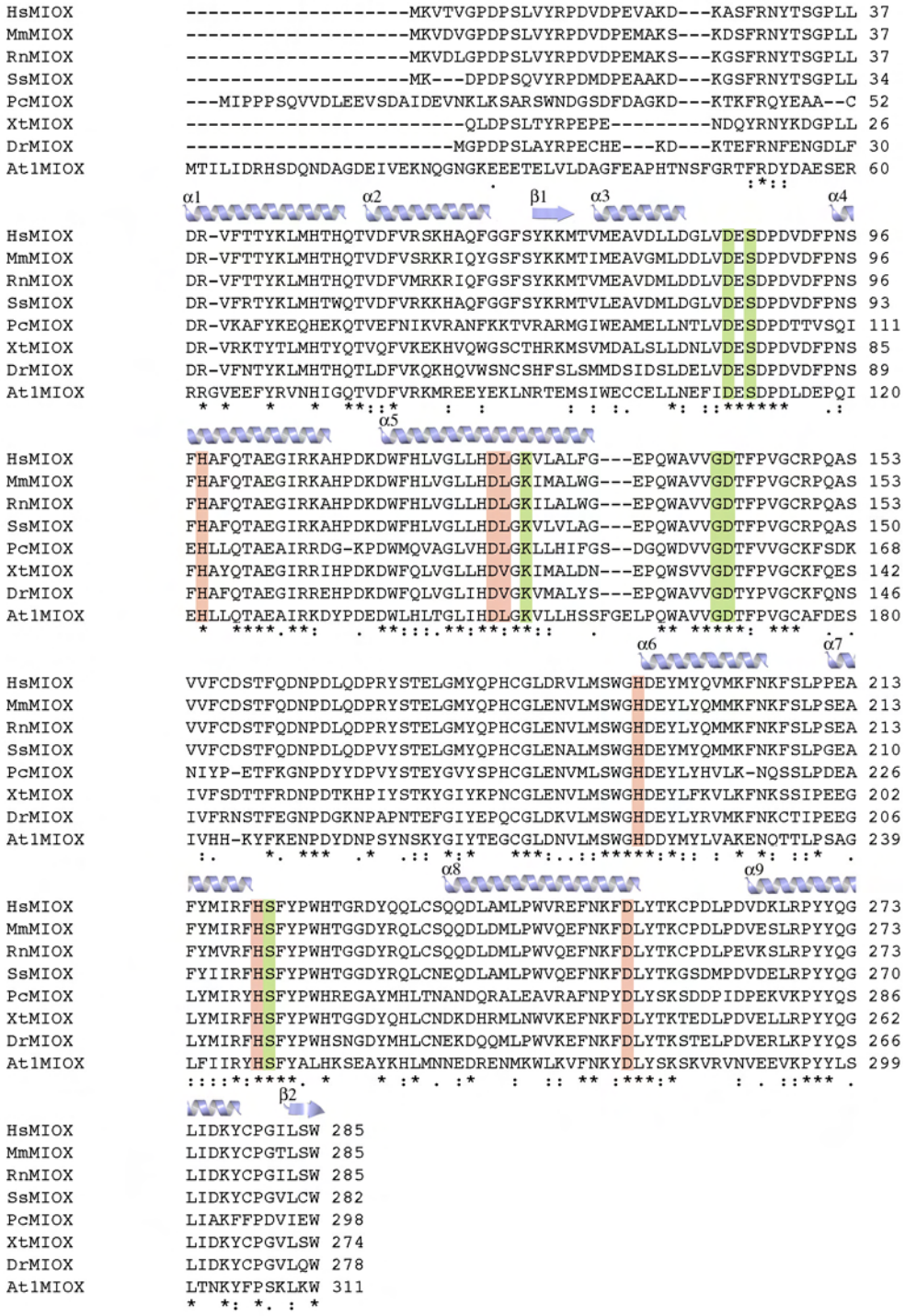

Figure S2. Assignment of *myo*-inosose-1 as bound species as opposed to *myo*-inositol. A SIGMAA-weighted (7) 2Fo-Fc map (blue) at 1σ and Fo-Fc (red) at -5σ is rendered from phases from a refinement where *myo*-inositol was present in the model. The final refined model of *myo*-inosose-1 is shown in gray for reference.

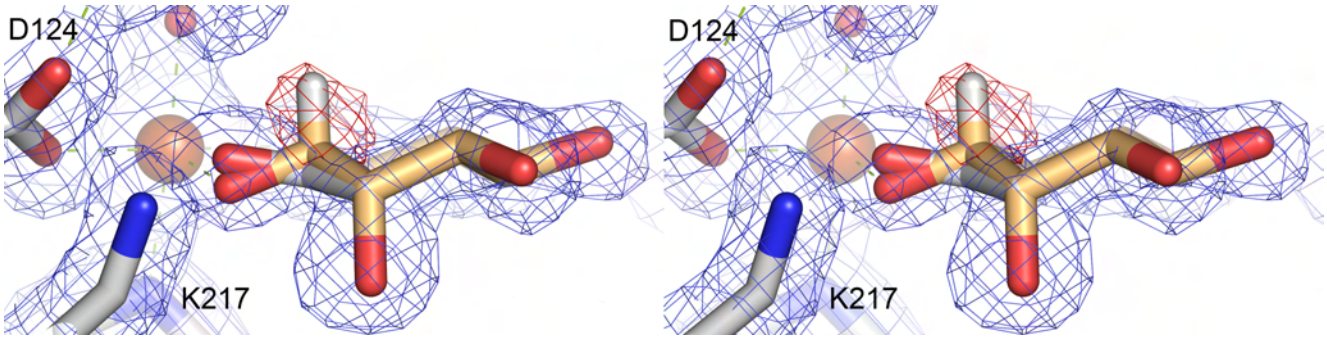

Figure S3. Modelling of a putative interaction between Asp[85] and the diiron cluster that can potentially be formed in the Lys[127]Ser mutant. Hs-MIOX in light brown, energy-minimised model of Lys[127]Ser mutant shown in green.

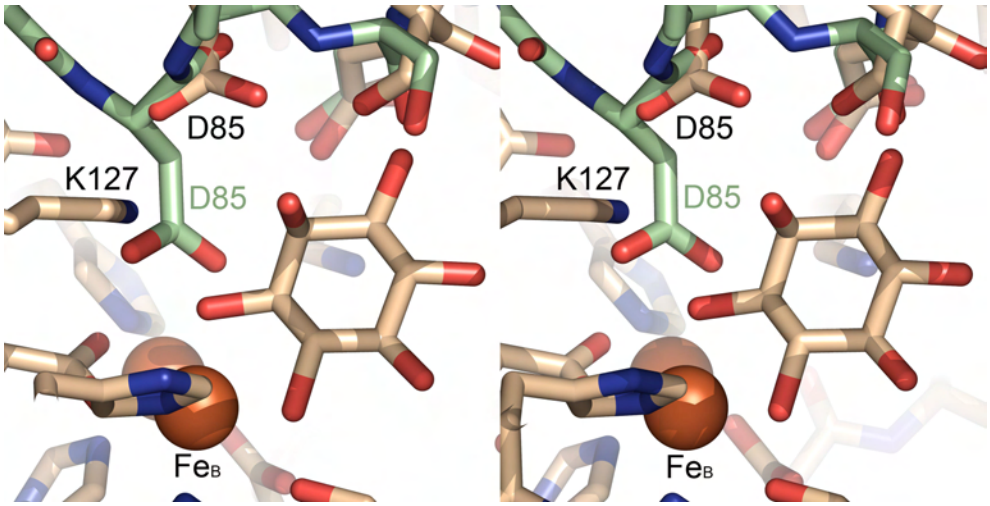

Figure S4. Experimental spectra of the mixed-valent state of human MIOX in the absence (upper panel, spectrum taken from Fig. 5A) and presence (lower panel, spectrum taken from Fig. 5B) of the substrate *myo*-inositol. Below each experimental spectrum there is a simulated spectrum with the following parameters for g-value and line width: Upper panel, sum of components I and II in a quantitative ratio 0.3/0.7. Component I, $g_{\|}$ = 1.96, $g_{\perp}$ =1.74, $L_{\|}$ = 25 G, $L_{\perp}$ = 160 G; component II, $g_{\|}$ = 1.94, $g_{\perp}$ = 1.72, $L_{\|}$ = 70 G, $L_{\perp}$ = 250 G. Both components were simulated with Gaussian line shape. Lower panel: simulated spectrum with g_x = 1.96, g_y = 1.82, g_z = 1.78; L_x = 25 G, L_y = 30 G, L_z = 60 G and Gaussian line shape.

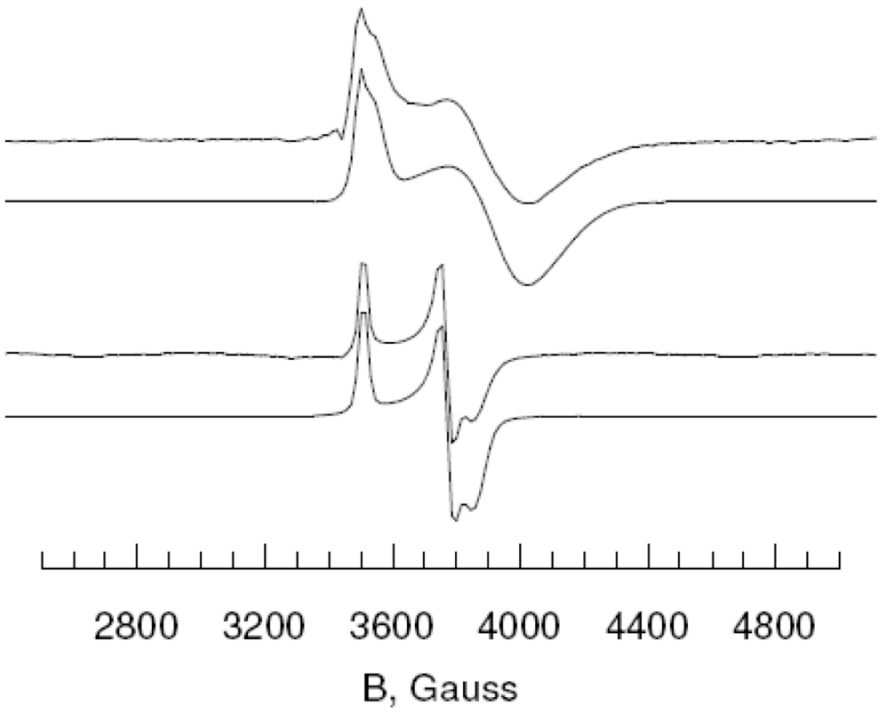

Figure S5. The EPR microwave saturation parameter $P_{1/2}$ of MIOX (o) and MIOX-inositol (●) as a function of the inverse absolute temperature. Saturation recovery data were collected at 5.5, 7.0 and 10.0 K. The exchange coupling constants, J ($H_{ex} = -2J \cdot S_1 \cdot S_2$), were estimated from the slopes as $\Delta = -3J$ and were determined to be ~20 cm^{-1} for MIOX and ~10 cm^{-1} for MIOX-inositol.

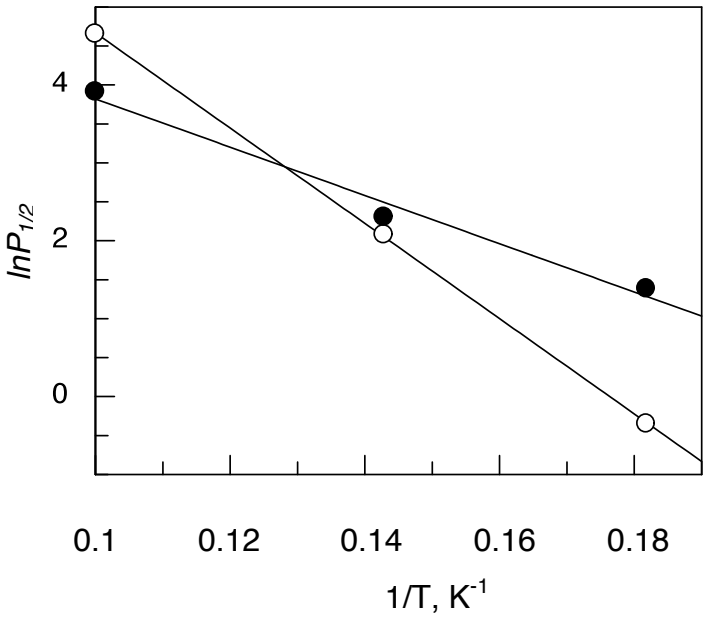

Table S1. Re-refinement statistics and quality of Mm-MIOX structure

Resolution (highest resolution shell) (Å)	42.6-2.0 (2.09-2.0)
R_{cryst} # (%)(highest resolution shell)	21.0 (30.4)
R_{free} # (%)(highest resolution shell)	25.5 (31.0)
RMS deviation from ideal geometry	
Bond lengths (Å)	0.005
Bond angles (°)	0.76
Average B-factors (Å^2)	56.5
Ramachandran plot (favored, allowed, outliers)(%)*	96.9, 3.1, 0
Wilson B-factor	26

* According to Molprobity (6)